lution of **10** (50 mg, 5.3×10^{-5} mol) in 2 mL of toluene was stirred under 1 atm H_2 at room temperature for 18 h. Hydrogen-saturated hexane (40 mL) was added and the resulting precipitate was collected, washed with hexane, and sucked dry to give **13** as a yellow powder (36 mg, 71%), mp 175–180 °C dec. The ^1H NMR (C_6D_6) of this powder indicated the presence of a 93:7 mixture of **13** and **10**.

For **13**: ^1H NMR (C_6D_6) δ 7.98 (m, 8 H, ortho protons of $P(C_6H_5)_3$ and ortho protons of one $P(C_6H_4\text{-}p\text{-}CH_3)_2$), 7.83 (dd, 2 H, J_{PH} = 11.2 Hz, J_{HH} = 8.2 Hz, ortho protons of one $P(C_6H_4\text{-}p\text{-}CH_3)_2$), 7.18–7.02 (m, 9 H, meta and para protons of $P(C_6H_5)_3$), 6.84 (d, 4 H, J_{HH} = 7.7 Hz, meta protons of $P(C_6H_4\text{-}p\text{-}CH_3)_2$), 4.85 (m, 2 H, C_5H_4P), 4.68 (m, 1 H, C_5H_4P), 4.40 (m, 1 H, C_5H_4P), 1.95 (s, CH_3), 1.93 (s, CH_3), −10.49 (td, $J_{PH} \approx J_{PH} \approx$ 17.4 Hz, J_{HH} = 3.7 Hz, 1 H, hydride), −12.93 (ddd, J_{PH} = 15.6 Hz, J_{PH} = 11.3 Hz, J_{HH} = 3.7 Hz, 1 H, hydride): ^{13}C NMR (CD_2Cl_2, 0.07 M $Cr(acac)_3$, 30 °C) δ 229.5 (br m, $Mo(CO)_3$), 177.4 (s, Ir(CO)), 141.8 (s, para, $P(C_6H_4\text{-}p\text{-}CH_3)_2$), 141.6 (s, para, $P(C_6H_4\text{-}p\text{-}CH_3)_2$), 135.0 (dd, $^1J_{PC}$ = 47.4 Hz, $^3J_{PC} \sim$ 7 Hz, ipso, $P(C_6H_5)_3$), 134.0 (d, J_{PC} = 9.2 Hz, ortho, $P(C_6H_5)_3$), 133.4 (d, J_{PC} = 12.2 Hz, ortho, $P(C_6H_4\text{-}p\text{-}CH_3)_2$), 131.8 (d, J_{PC} = 12.2 Hz, ortho, $P(C_6H_4\text{-}p\text{-}CH_3)_2$), 130.0 (s, para, $P(C_6H_5)_3$), 129.3 (d, J_{PC} = 9.2 Hz, meta, $P(C_6H_4\text{-}p\text{-}CH_3)_2$), 129.0 (d, J_{PC} = 9.2 Hz, meta, $P(C_6H_4\text{-}p\text{-}CH_3)_2$), 127.7 (d, J_{PC} = 6.1 Hz, meta, $P(C_6H_5)_3$), 92.1 (d, J_{PC} = 9.2 Hz, 1 C, C_5H_4P), 91.8 (d, J_{PC} = 12.2 Hz, 1 C, C_5H_4P), 90.7 (d, J_{PC} = 6.1 Hz, 1 C, C_5H_4P), 89.6 (d, J_{PC} = 6.1 Hz, 1 C, C_5H_4P), 59.6 (d, J_{PC} = 64.2 Hz, C_1 of C_5H_4P), 21.0 (s, CH_3), ipso carbons of $P(C_6H_4\text{-}p\text{-}CH_3)_2$ not observed. At −30 °C the Mo carbonyls appeared as three equal intensity singlets at δ 233.9, 227.6, and 224.9 ^{31}P NMR (CD_2Cl_2, 0.07 M $Cr(acac)_3$) AB quartet, δ 14.0 (J_{PP} = 312 Hz, $P(C_6H_5)_3$), 9.0 (J_{PP} = 312 Hz, $(C_6H_4\text{-}p\text{-}CH_3)_2PC_5H_4$); IR (THF) 2100 (w, ν_{Ir-H}), 1992 (m), 1941 (s), 1874 (m), 1853 (m) cm^{-1}. IR (THF) of $D_2(CO)[P(C_6H_5)_3]IrMo(CO)_3[\eta^5\text{-}C_5H_4P(C_6H_4\text{-}p\text{-}CH_3)_2]$ 2015 (m), 1946 (s), 1876 (m), 1852 (m), 1497 (w, ν_{Ir-D}) cm^{-1}.

High-Pressure Reactions. All high-pressure reactions were performed in a 22-mL stainless steel Parr bomb. Solvents, substrates, and organometallic compounds were added to the bomb in an inert atmosphere glovebox. The bomb was surrounded by an aluminum heating block that was maintained at constant temperature by remote control. Samples of the reaction solution were obtained by cooling the bomb to −196 °C (to avoid loss of solvent), releasing the pressure, and taking the bomb into the glovebox where it was opened. Samples of the solution were then removed and analyzed by IR spectroscopy.

Attempted Cyclohexene Hydrogenation. Samples from attempted hydrogenation of cyclohexene were removed from the bomb as described above and bulb-to-bulb distilled on a vacuum line to separate nonvolatile materials. The solution was analyzed by gas chromatography on a 20 ft × $^1/_8$ in 20% UCON-50-HB-280X column at 155 °C.

Attempted CO Reduction Experiments. In order to analyze for formation of methane as a CO reduction product, the outlet of the bomb was connected to an evacuated vacuum line via copper tubing. The bomb was cooled to −78 °C, and the gases in the bomb were allowed to expand into the vacuum line; samples were removed by syringe and analyzed by gas chromatography. A 10 ft × $^1/_8$ in Poropak Q column at room temperature was used for CH_4 analysis. The bomb was then taken into the glovebox, and samples were removed for IR spectroscopy and for analysis for CH_3OH by gas chromatography. A 20 ft × $^1/_8$ in 20% UCON-50-HB-280X column at 135 °C was used for methanol analysis. The sample was bulb-to-bulb distilled on a vacuum line and analyzed by gas chromatography for CH_3OH. When toluene was used as a solvent, it was extracted with 0.20–0.25 mL of H_2O to concentrate any CH_3OH which might have formed, and this aqueous solution was also analyzed for CH_3OH by gas chromatography. Detection limits were 5% for CH_3OH and 1% for CH_4.

Acknowledgment. Support from the Division of Basic Energy Sciences of the Department of Energy is gratefully acknowledged. F.N. wishes to thank CNRS for financial support and NATO for a fellowship. We thank Dr. Stanley W. Polichnowski and Ms. Norma Lafferty of the Tennessee Eastman Co. for carrying out the high-pressure infrared experiment. We also thank Professor M. D. Rausch for informing us of some of his results prior to publication.

Registry No. 1, 83334-37-6; **2**, 87801-08-9; **3**, 87828-72-6; **4**, 87801-09-0; **5**, 87801-10-3; **6**, 87801-11-4; **7**, 87801-12-5; **8**, 87801-13-6; **9**, 87801-14-7; **10**, 87801-15-8; **11**, 87801-16-9; **11**-d_2, 87801-21-6; **12**, 87801-17-0; **12**-d_2, 87801-22-7; **13**, 87801-18-1; **13**-d_2, 87801-23-8; $[(C_6H_4\text{-}p\text{-}CH_3)_2PCH_2]_2$, 70320-30-8; $LiP(C_6H_4\text{-}p\text{-}CH_3)_2$, 39952-43-7; $[(C_2H_4)_2RhCl]_2$, 12081-16-2; $[(CO)_2RhCl]_2$, 14523-22-9; $Mo(CO)_6$, 13939-06-5; $LiC_5(CH_3)_4P(C_6H_4\text{-}p\text{-}CH_3)_2Mo(CO)_5$, 87801-19-2; $Li(CO)_3MoC_5(CH_3)_4P(C_6H_4\text{-}p\text{-}CH_3)_2$, 87801-20-5; $(CO)_2IrCl(H_2NC_6H_4\text{-}p\text{-}CH_3)$, 14243-22-2; di-*p*-tolylchlorophosphine, 1019-71-2; 1,2-dichloroethane, 107-06-2; lithium 1-(di-*p*-tolylphosphino)-2,3,4,5-tetramethylcyclopentadienide, 87781-75-7; 1,2,3,4-tetramethylcyclopentadiene, 4249-10-9; lithium tetranaphthylcyclopentadienide, 87781-76-8; 1-(di-*p*-tolylphosphino)-2,3,4,5-tetramethylcyclopentadiene, 87781-77-9; cyclohexene, 110-83-8.

A Reversible Chemical Reaction in a Single Crystal. The Dimerization of $(\eta^5\text{-}C_5H_5)Co(S_2C_6H_4)$

Edward J. Miller, Thomas B. Brill,* Arnold L. Rheingold,* and William C. Fultz

Contribution from the Department of Chemistry, University of Delaware, Newark, Delaware 19711. *Received April 15, 1983*

Abstract: A reversible single-crystal chemical reaction was discovered to occur when a crystal of cyclopentadienyl(*o*-dithiobenzene)cobalt, I, converts at room temperature to produce a crystal of the dimer, II. Compound II reverts to I at 150 °C with retention of crystallinity. Dissolution of II in noncomplexing solvents also yields I. The structures of I and II were determined by single-crystal X-ray crystallography. I crystallizes in the space group $P2_1/c$ (No. 14), a = 15.040 (2) Å, b = 9.315 (1) Å, c = 16.429 (3) Å, β = 110.27 (1)°, Z = 8, and R = 0.060. Compound II crystallizes in the space group $P2_1/c$, a = 9.243 (2) Å, b = 11.362 (2) Å, c = 10.422 (2) Å, β = 112.51 (2)°, Z = 2, and R = 0.042. Covalent Co–S bonds bridge the metal centers in II. However, differential scanning calorimetry measurements reveal that ΔH = 18.9 kJ mol^{-1} for II → I, which suggests that the crystal packing and molecular deformation forces delicately balance the bridging Co–S bond energies in II.

Authentic examples of *reversible* chemical reactions occurring in a single crystal are sublimely rare. Chemical reactions in the solid state almost always consist of irreversible changes, such as polymerization[1–4] or thermal decomposition.[5–8] Another type of solid-state event, the reconstructive solid-phase–solid-phase transformation, generally results from a physical change in the

(1) Elgavi, A.; Green, B. S.; Schmidt, G. M. J. *J. Am. Chem. Soc.* **1973**, *95*, 2058–9.
(2) Cohen, M. J.; Garito, A. F.; Heeger, A. J.; MacDiarmid, A. G.; Mikulski, C. M.; Saran, M. S.; Kleppinger, J. *J, Am. Chem. Soc.* **1976**, *98*, 3844–48.
(3) Nakaniski, H.; Jones, W.; Thomas, J. M. *Chem. Phys. Lett.* **1980**, *71*, 44–48.
(4) For review, see Gavezzotti, A.; Simonetta, M.; *Chem. Rev.* **1982**, *82*, 1–13.
(5) Paul, I. C.; Curtin, D. Y. *Acc. Chem. Res.* **1973**, *6*, 217–225.
(6) Dubovitskii, F. I.; Korsunskii, B. L. *Russ. Chem. Rev.* (*Engl. Transl.*) **1981**, *50*, 958–978.

0002-7863/83/1505-7580$01.50/0

crystal structure symmetry rather than a chemical reaction, but it is frequently reversible.[9]

The interface between these two solid processes, in which the reversibility of a phase transition and the molecularity of a genuine chemical reaction are incorporated, would be extremely intriguing. Touching on this interface are compounds that occasionally exhibit conformational polymorphism.[10] Conformational polymorphs have the characteristics of some phase transitions, as they can be reversible solid-state processes. Substituted benzylideneanilines[10,11] and the energetic material, octahydro-1,3,5,7-tetranitro-1,3,5,7-tetrazocine (HMX),[12] among others,[4] exhibit conformational polymorphism. Several inorganic[13,14] and organometallic[15] complexes have been shown recently to undergo *irreversible* solid-phase transformations in which a molecular property, such as the color or coordination number, is modified.

In this paper we report a study of what appears to be a unique example of a completely reversible solid-phase chemical reaction. This is the dimerization (reaction 1) of $(\eta^5\text{-}C_5H_5)Co(S_2C_6H_4)$, I, which takes place between two crystalline phases having the

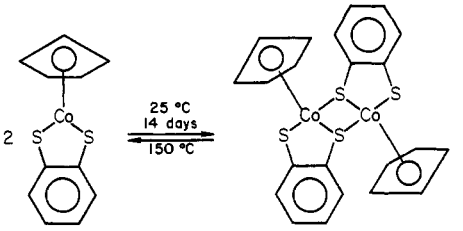

(1)

I II

space group $P2_1/c$. The event was discovered by a combination of nuclear quadrupole resonance and X-ray crystallographic techniques. The NQR spectrum of I was observed to change drastically with time suggesting that a major structural alteration had taken place. Crystallographic characterization of both phases (I and II) has been achieved. After allowing one of the data crystals used to determine the structure of I to remain at room temperature, we were intrigued to find that it had converted to the structure of II. Newly formed covalent Co–S bonds bridge the metal centers in II. However, II is stabilized at room temperature by the presence of the crystal lattice and reverts to a single crystal of I upon heating. Crystals of II also dissolve in non-complexing organic solvents to produce a solution of I.

Experimental Section

General. *o*-Benzenedithiol[16] and $(\eta^5\text{-}C_5H_5)Co(S_2C_6H_4)$[17] (I) were prepared according to known procedures. The dimer $[(\eta^5\text{-}C_5H_5)Co(S_2C_6H_4)]_2$ (II) forms when the moisture-free monomer is allowed to sit at room temperature for several weeks. However, it was subsequently discovered that exceptionally well-formed prisms of I could be obtained by sublimation of I or II. Crystals of I formed in this manner are very slow to dimerize, probably because they lack defects which might act as nucleation sites for the conversion. It was also found that crystals of II could be obtained when a CH_2Cl_2 solution of I or II slowly evaporated over a period of 24 h. On the other hand, more rapid evaporation (such as rotovaping a CH_2Cl_2 solution of I or II) produces crystals of I. It is frequently found that the crystal structure adopted by a material depends on the rate of evaporation of the crystallizing medium.[18]

Compounds I and II are intensely purple. Prominent IR modes (cm^{-1}) of I: 743 s, 841 s, 1408 m, 1417 m; of II: 755s, 820s, 834s, 1412m, 1419m, 1438m cm^{-1}. UV–vis absorptions of I in CH_2Cl_2: 570 ± 3 (ϵ 1.1×10^4), 290 ± 3 nm (ϵ 3.1×10^4). UV photolysis of the solid appears to have no effect on reaction 1.

The enthalpy change of reaction 1 was measured on a Du Pont 990 differential scanning calorimeter (DSC) with an N_2 atmosphere and a 10 °C/min heating rate. Indium metal was used for calibration. A single endotherm was observed, the area under which was calculated by integration of the analog output. The infrared spectra were recorded on a Nicolet 60SX FT-IR spectrometer with neat samples between NaCl plates. The NQR spectra were recorded at 20 °C on a Wilks NQR-1A superregenerative oscillator spectrometer. The resonance frequencies are accurate to ±0.005 MHz.

Crystal Structure Determinations. Crystals of I were grown by evaporation of a hexane/CH_2Cl_2 solution. (50/50 v/v). Crystals of II resulted when crystals of I sat for several weeks. X-ray diffraction data were collected on a Nicolet R3 diffractometer. Table I summarizes the unit cell parameters and details of data collection for the crystallographic studies of I and II. Unless otherwise stated, the following pertains to both structure determinations. The crystals were affixed to fine glass fibers with urethane varnish, which also was used to coat the crystals to provide a barrier to the atmosphere. Systematic absences uniquely determined the space group in both cases. Corrections to the intensity data were made for Lp effects and for absorption; empirical ψ-scan techniques were used (maximum transmission, minimum transmission: I, 0.779, 0.690; II, 0.223, 0.197). Due to the conversion of I → II which takes place slowly at room temperature, three crystals of I were used during data collection, each being replaced when check reflection intensities dropped by approximately 10%. These same check reflection intensities were used to correct for decay and to provide scale factors for merging the data from the three crystals.

The positions of the Co and S atoms were obtained from solutions derived from SHELXTL direct methods software. The remaining non-hydrogen atoms were located in subsequent difference Fourier syntheses. All hydrogen atoms in II were found and refined, whereas in I, the hydrogen atoms were positioned in idealized locations (d(C–H) = 0.96 Å) by using an updated "riding" model. Least-squares refinement using anisotropic thermal parameters for all non-hydrogen atoms converged at the final residuals given in Table I; Table II provides the atomic coordinates for I, and Table III, the same for II. Tables of hydrogen atom coordinates, atomic thermal parameters, and F_o and F_c are available as supplementary material.

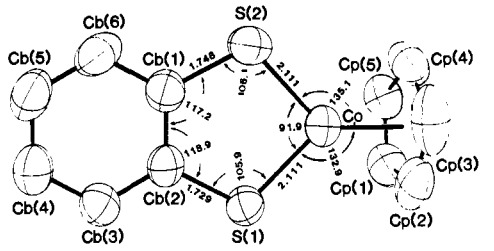

Figure 1. Molecular structure (50% probability ellipsoids) and labeling scheme for I, the monomeric form of $(\eta^5\text{-}C_5H_5)Co(S_2C_6H_4)$. One of two independent, but not significantly different, molecules of I is depicted.

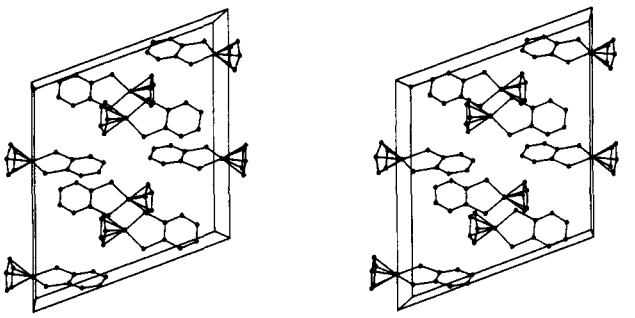

Figure 2. Unit cell packing diagram for I viewed along the *b* crystallographic axis. This packing diagram is drawn to illustrate the relationship between the molecules shown in Figure 3.

Results and Discussion

Characterization of the Structures. Selected bond distances and angles from I and II are presented in Tables IV and V, respectively. The monomeric form of $(\eta^5\text{-}C_5H_5)Co(S_2C_6H_4)$ crystallizes as pairs of crystallographically independent, well-separated molecules. The molecular structure and labeling scheme

(7) Young, D. A. "Decomposition of Solids"; Pergamon Press: New York, 1966.
(8) Bamford, C. H.; Tipper, C. F. H. In "Comprehensive Chemical Kinetics,"; Elsevier: New York, 1980; Vol. 22.
(9) Rao, C. N. R. "Modern Aspects of Solid State Chemistry"; Plenum Press: New York, 1970; p 589 ff.
(10) Bernstein, J.; Hagler, A. T. *J. Am. Chem. Soc.* **1978**, *100*, 673–680.
(11) Bar, I.; Bernstein, J. *J. Phys. Chem.* **1982**, *86*, 3223–3231.
(12) Brill, T. B.; Reese, C. O. *J. Phys. Chem.* **1980**, *84*, 1376–1380.
(13) Foxman, B. M.; Goldberg, P. L.; Mazurek, H. *Inorg. Chem.* **1981**, *20*, 4368–75.
(14) Foxman, B. M.; Cheng, K. *J. Am. Chem. Soc.* **1977**, *99*, 8102–8103.
(15) Etter, M. C.; Siedle, A. R. *J. Am. Chem. Soc.* **1983**, *105*, 641–43.
(16) Ferretti, A. *Org. Synth.* **1973**, *5*, 419–421.
(17) Heck, R. F. *Inorg. Chem.* **1968**, *7*, 1513–1516.
(18) Brill, T. B.; Karpowicz, R. J. *J. Phys. Chem.* **1982**, *86*, 4260–4265.

Table I. Experimental Data for the X-ray Diffraction Study of I and II

	I (monomer)	II (dimer)
(a) Crystal Parameters at 24 °C[a]		
crystal system	monoclinic	monoclinic
space group	$P2_1/c$ [C_{2h}^5; No. 14]	$P2_1/c$
a, Å	15.040 (2)	9.243 (2)
b, Å	9.315 (1)	11.362 (2)
c, Å	16.429 (3)	10.422 (2)
β, deg	110.27 (1)	112.51 (2)
V, Å^3	2159.1 (6)	1031.2 (3)
Z	8	2
M_r	264.23	528.46
ρ(calcd)	1.63	1.73
μ(Mo Kα)	19.13	20.42
(b) Measurement of Data		
diffractometer	Nicolet R3	
monochrometer	highly oriented graphite	
crystal dimensions, mm	0.05 × 0.20 × 0.50	0.30 × 0.30 × 0.30
reflctns measd	±h,k,l	±h,k,l
2θ range	3–45 (2θ/θ)	3–50 (2θ/θ)
scan speed, deg/min	3.5	3.5
reflctns collected	3032	2042
unique reflctns:	2620	1788
unique reflctns used in refinement	2163 [$F = 2\sigma(F)$]	1453 [$F = 3\sigma(F)$]
no. of parameters refined	254 (8.5:1 ratio)	164 (8.9:1 ratio)
std reflctns	3/97 (10% decay)	3/97 (no decay)
R_F, R_{wF} (%)[b]	6.0, 5.4	4.2, 3.9
GOF[c]	1.447	1.183
highest peak, final difference map, e$^-$/Å^3	0.56	0.53
max shift to error in final cycle	0.107	0.038

[a] Unit cell parameters were obtained from the angular settings of the unresolved Mo Kα components of 25 reflections with $20° \leq 2\theta \leq 30°$. [b] $R_F = \Sigma||F_o| - |F_c||/\Sigma|F_o|$; $R_{wF} = \{\Sigma_w(|F_o| - |F_c|)^2/\Sigma_w|F_o|^2\}^{1/2}$. [c] GOF = $\{\Sigma_w(|F_o| - |F_c|)^2/(N_o - N_v)\}^{1/2}$, where N_o = number of observations and N_v = number of variables.

Table II. Final Positional Parameters for the Non-Hydrogen Atoms in I (Monomer)

atom	x	y	z
(a) Molecule 1			
Co	0.00680 (6)	0.48314 (9)	0.65728 (6)
S(1)	−0.0648 (1)	0.3087 (2)	0.5803 (1)
S(2)	−0.1215 (1)	0.5734 (2)	0.6584 (1)
Cp(1)	0.1343 (5)	0.4823 (9)	0.6368 (5)
Cp(2)	0.1480 (5)	0.4054 (9)	0.7115 (7)
Cp(3)	0.1194 (5)	0.4970 (10)	0.7694 (6)
Cp(4)	0.0991 (5)	0.6347 (9)	0.7298 (5)
Cp(5)	0.1079 (5)	0.6214 (8)	0.6485 (4)
Cb(1)	−0.2115 (5)	0.4594 (6)	0.5956 (4)
Cb(2)	−0.1841 (5)	0.3382 (7)	0.5599 (4)
Cb(3)	−0.2535 (4)	0.2438 (7)	0.5104 (4)
Cb(4)	−0.3470 (5)	0.2718 (9)	0.4951 (5)
Cb(5)	−0.3734 (5)	0.3902 (9)	0.5293 (5)
Cb(6)	−0.3066 (5)	0.4858 (8)	0.5787 (5)
(b) Molecule 2			
Co′	0.48075 (6)	0.53686 (9)	0.80943 (6)
S(1)′	0.5743 (1)	0.6410 (2)	0.9209 (1)
S(2)′	0.5919 (1)	0.4786 (2)	0.7654 (1)
Cp(1)′	0.3513 (4)	0.6144 (8)	0.8005 (5)
Cp(2)′	0.3675 (5)	0.4845 (9)	0.8431 (5)
Cp(3)′	0.3814 (5)	0.3822 (8)	0.7869 (8)
Cp(4)′	0.3726 (5)	0.4519 (10)	0.7086 (6)
Cp(5)′	0.3552 (5)	0.5901 (8)	0.7182 (5)
Cb(1)′	0.6954 (5)	0.5390 (6)	0.8446 (4)
Cb(2)′	0.6864 (4)	0.6136 (6)	0.9163 (4)
Cb(3)′	0.7680 (5)	0.6619 (8)	0.9809 (5)
Cb(4)′	0.8558 (6)	0.6359 (9)	0.9772 (6)
Cb(5)′	0.8640 (5)	0.5606 (9)	0.9062 (7)
Cb(6)′	0.7848 (5)	0.5113 (8)	0.8411 (6)

Table III. Final Positional Parameters for the Non-Hydrogen Atoms in II (Dimer)

atom	x	y	z
Co	−0.05199 (6)	0.51560 (4)	0.13334 (5)
S(1)	0.1956 (1)	0.48040 (9)	0.2790 (1)
S(2)	0.0365 (1)	0.63236 (8)	0.0075 (1)
C(1)	0.3004 (4)	0.5962 (3)	0.2431 (1)
C(2)	0.2307 (4)	0.6650 (3)	0.1253 (4)
C(3)	0.3138 (5)	0.7565 (3)	0.0955 (4)
C(4)	0.4659 (5)	0.7794 (4)	0.1825 (5)
C(5)	0.5353 (5)	0.7113 (4)	0.2972 (5)
C(6)	0.4550 (5)	0.6209 (5)	0.3283 (5)
C(7)	−0.2471 (5)	0.4486 (4)	0.1599 (5)
C(8)	−0.2898 (5)	0.5451 (5)	0.0697 (5)
C(9)	−0.2090 (6)	0.6426 (5)	0.1438 (6)
C(10)	−0.1144 (6)	0.6064 (5)	0.2767 (5)
C(11)	−0.1372 (6)	0.4836 (6)	0.2883 (5)

Table IV. Selected Bond Distances and Bond Angles for I (Monomer)

	molecule 1	molecule 2
(a) Bond Distances (Å)		
Co–S(1)	2.111 (2)	2.119 (2)
Co–S(2)	2.111 (2)	2.109 (2)
Co–CNT[a]	1.643 (2)	1.648 (2)
S(1)–Cb(2)	1.729 (7)	1.732 (3)
S(2)–Cb(1)	1.748 (6)	1.740 (6)
Cp ring ⟨av⟩	1.398	1.379
Cb ring ⟨av⟩	1.379	1.389
(b) Bond Angles (deg)		
S(1)–Co–S(2)	91.9 (1)	92.6 (1)
S(1)–Co–CNT	132.9 (1)	134.7 (2)
S(2)–Co–CNT	135.1 (2)	132.6 (6)
Co–S(1)–Cb(2)	105.9 (2)	105.1 (3)
Co–S(2)–Cb(1)	106.1 (2)	105.7 (3)
S(1)–Cb(2)–Cb(1)	118.9 (5)	118.9 (4)
S(2)–Cb(1)–Cb(2)	117.2 (5)	117.6 (5)

[a] CNT = centroid of η^5-C_5H_5 ring.

Table V. Selected Bond Distances and Bond Angles for II (Dimer)

(a) Bond Distances (Å)			
Co–S(1)	2.246 (1)	S(1)–C(1)	1.757 (4)
Co–S(2)	2.230 (1)	S(2)–C(6)	1.783 (3)
Co–S(2)′	2.272 (1)	Cb ring ⟨av⟩	1.382
Co–CNT[a]	1.698 (3)	Cp ring ⟨av⟩	1.399
Co–Co′	3.2893 (4)		
(b) Bond Angles (deg)			
S(1)–Co–S(2)	89.73 (4)	Co–S(2)–Co′	93.94 (4)
S(1)–Co–S(2)′	90.31 (4)	Co–S(1)–C(1)	103.0 (1)
S(2)–Co–S(2)′	86.09 (4)	Co–S(2)–C(2)	102.6 (1)
CNT–Co–S(1)	123.4 (1)	S(1)–C(1)–C(2)	120.2 (3)
CNT–Co–S(2)	126.9 (1)	S(2)–C(2)–C(1)	119.7 (3)
CNT–Co–S(2)′	128.3 (1)		
(c) Torsion Angles (deg)			
CNT–Co–S(2)–Co′	−136.5	CNT–Co–S(2)–C(2)	114.4
CNT–Co–S(1)–C(1)	−117.6		

[a] CNT = centroid of η^5-C_5H_5 ring.

for one of the independent molecules are given in Figure 1, and a unit cell packing diagram is given in Figure 2. Differences between the independent molecules are slight and without chemical significance. The molecular structure of the monomer is closely similar to that found for $(\eta^5\text{-}C_5H_5)Co[S_2C_2(CN)_2]$[19] (III). The

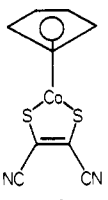

III

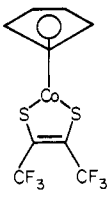

IV

Table VI. Least-Squares Planes for I (Monomer)[a,b]

atoms	dev	atoms	dev
Plane I:	$0.0695x - 0.5219y + 0.8501z = 6.8176$		
Co	−0.0094	*Cb(1)*	−0.0024
S(1)	0.0102	*Cb(2)*	−0.0066
S(2)	0.0082	CNT[c]	−0.0309
Plane II:	$0.9661x + 0.2479y + 0.0722z = 3.6410$		
Cp(1)	0.0082	*Cp(4)*	0.0038
Cp(2)	−0.0058	*Cp(5)*	−0.0075
Cp(3)	0.0013	CNT	−0.0130
	(dihedral I/II = 90.1°)		
Plane III:	$-0.0908x + 0.8611y - 0.5003z = -1.6883$		
Co'	−0.0216	*Cb(1)'*	−0.0089
S(1)'	0.0217	*Cb(2)'*	−0.0117
S(2)'	0.0205	CNT'	−0.1099
Plane IV:	$0.9817x + 0.1904y + 0.0054z = 6.0172$		
Cp(1)'	−0.0007	*Cp(4)'*	−0.0027
Cp(2)'	−0.0010	*Cp(5)'*	0.0027
Cp(3)'	0.0022	CNT	0.0046
	(dihedral III/IV = 85.9°)		

[a] Orthonormal coordinates. [b] Italicized atoms used to construct plane. [c] CNT = centroid of η^5-C_5H_5 ring.

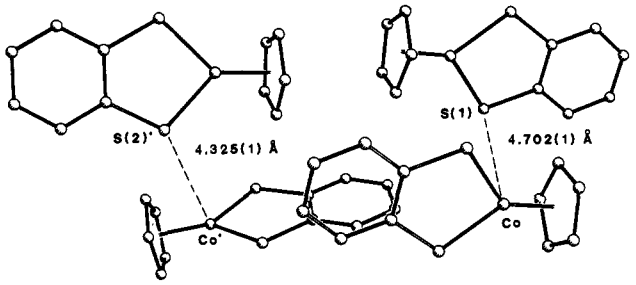

Figure 3. Nearest intermolecular Co···S distance in I. All Co–S intermolecular interactions less than 5.2 Å occur between molecules of the same crystallographically independent unit. All of these distances exceed the sum of the Co and S van der Waals radii, but feasibly position the molecules for dimerization.

CoS_2C_2 metallacycle in I is nearly planar (See Table VI) and perpendicular to the η^5-C_5H_5(Cp) ring (dihedral angle for molecule A = 90.1°, molecule B = 85.9°). In III[18] the metallacycle is also nearly planar with a dihedral angle of 88.6°. The metallacycle does not display a pattern of bond angles and distances that would support a case for significant circumannular electron delocalization as may exist in the nitrogen analogue $(\eta^5\text{-}C_5H_5)Co[(NH)_2C_6H_4]$.[19] The S–C bond distances in I (1.737 (4) Å ⟨average⟩) are *longer* than in III (1.702 (7) Å), which, even with its shorter S–C bond distances, is believed not to contain significant C–S multiple bond character.[19,21] Additionally, the range and pattern of C–C bond distances found in the phenylene ring of I are not those required to describe the ligand as a dithioquinone. The central S(1)–Co–S(2) angle of I (92.3 (1)° ⟨average⟩) is similar to that found in III[19] (93.2 (1)°) and in IV[12] (92.2°).

When packing in the crystal lattice, the molecules of I adopt "head-to-tail" arrangements of pairs of independent molecules, with the nearest contacts being between identical molecules in different equivalent positions. The intermolecular interaction in the monomer, I, showing the shortest Co···S contacts is depicted in Figure 3. Although the contact distances, Co···S(1) = 4.702 (1) Å and Co···S(2) = 4.325 (1) Å, are very long, the relative positions of the molecule resemble the heavy-atom structure of the dimeric form, II. Nonetheless, upon dimerization, profound changes occur in the molecular architecture. The structure and

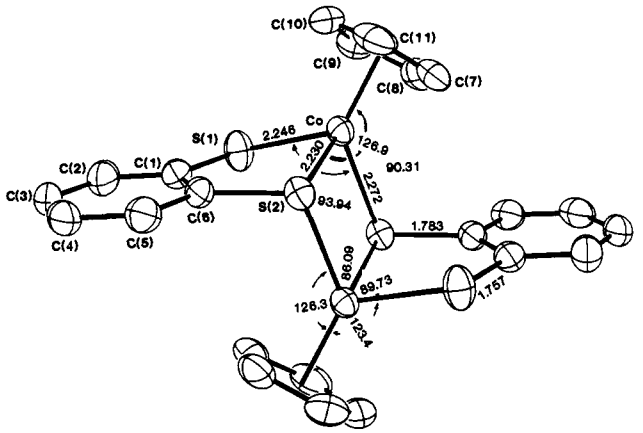

Figure 4. Molecular structure (50% probability ellipsoids) and labeling scheme for II, the dimeric form of $(\eta^5\text{-}C_5H_5)Co(S_2C_6H_4)$, i.e., $[\eta^5\text{-}C_5H_5)Co(S_2C_6H_4)]_2$.

Table VII. Least-Squares Planes for II (Dimer)[a,b]

atoms	dev	atoms	dev
Plane I:	$0.9401x - 0.1852y + 0.2861z = -1.0520$		
Co	0.0000	*S(2)*	0.0000
Co'	0.0000	*S(2)'*	0.0000
Plane II:	$0.7430x - 0.1971y - 0.6396z = -4.1891$		
C(7)	−0.0080	*C(10)*	0.0020
C(8)	0.0092	*C(11)*	0.0037
C(9)	−0.0069	CNT	−0.0003
	(dihedral I/II = 56.6°)		
Plane III:	$-0.3214x + 0.6311y + 0.7059z = 4.4846$		
C(1)	0.0047	*C(6)*	−0.0014
C(2)	−0.0033	S(1)	−0.0124
C(3)	−0.0015	S(2)	−0.0864
C(4)	0.0050	Co	0.4664
C(5)	−0.0035		
	(dihedral I/III = 102.5°, II/III = 144.6°)		
Plane IV:	$-0.2211x + 0.7052y + 0.6737z = 5.1296$		
Co	0.1598	*C(1)*	0.0711
S(1)	−0.1572	*C(6)*	0.0929
S(2)	−0.1666		
	(dihedral I/IV = 98.4°, II/IV = 137.2°, III/IV = 7.4°)		
Plane V:	$-0.0403x + 0.7831y + 0.6206z = 5.5822$		
Co	0	C(1)	0.5322
S(1)	0	C(6)	0.5594
S(2)	0		
Plane VI:	$-0.3576x + 0.6248y + 0.6941z = 4.3466$		
C(1)	0.0045	*S(1)*	−0.0101
C(6)	−0.0044	*S(2)*	0.0101
	(dihedral V/VI = 20.9°)		
Plane VII:	$0.7763x - 0.1817y - 0.6036z = -1.0323$		
S(1)	0	*S(2)'*	0
S(2)	0		
	(dihedral II/VII = 2.9°)		

[a] Orthonormal coordinates. [b] Italicized atoms used to construct planes.

labeling scheme for the dimeric form, II, are shown in Figure 4, and a stereoview of the unit cell packing is given in Figure 5. The Co atom environment is transformed from a two-legged piano-stool geometry in I to a three-legged version in II. The η^5-C_5H_5 ring undergoes tilting of about 45° relative to the S(1)–Co–S(2) plane when I converts to II. Whereas in I the metallacycle is nearly planar (max dev = 0.02 Å), a folding occurs in II along the S(1)···S(2) vector (Table VII). A dihedral angle of 20.9° relates the S(1)–C(1)–C(6)–S(2) and S(1)–Co–S(2) planes in II. Despite this folding, the differences in the S–C bond distances in I and II are not chemically significant, which further suggests that little

(19) Churchill, M. R.; Fennessey, J. P. *Inorg. Chem.* **1968**, *7*, 1123–1129.
(20) Rheingold, A. L.; Fultz, W. C.; Brill, T. B.; Landon, S. J. *J. Crystallogr. Spectrosc. Res.* **1983**, *13*, 317–323. Gross, M. E.; Ibers, J. A.; Trogler, W. C. *Organometallics* **1982**, *1*, 530–535.
(21) Miller, E. J.; Brill, T. B. *Inorg. Chem.* **1983**, *22*, 2392–2398.
(22) Baird, H. W.; White, B. M. *J. Am. Chem. Soc.* **1966**, *88*, 4744–4746.

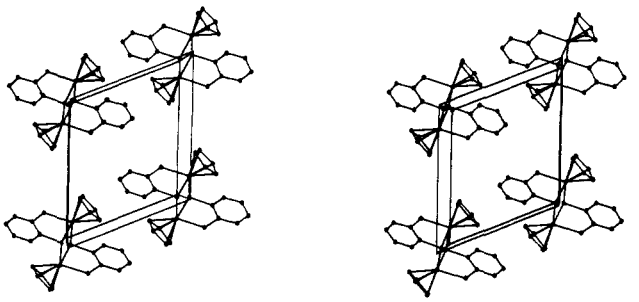

Figure 5. Unit cell packing diagram for II along the *b* crystallographic axis.

Table VIII. ^{59}Co NQR Data for I and II at 20 °C[a]

complex	$\nu(^7/_2 \leftrightarrow {}^5/_2)$, MHz	$\nu(^5/_2 \leftrightarrow {}^3/_2)$, MHz	e^2Qq/h, MHz	η
I	31.618 (4)	19.979 (6)	152.10	0.531
	31.445 (4)	19.878 (6)	150.89	0.514
II	27.690 (5)	18.204 (3)	129.65	0.182

[a] Parenthetical numbers are signal-to-noise ratios.

electron delocalization occurs in the metallacycle of either I or II.[21]

The Co–S distances in II are nearly equidistant: Co–S(1) = 2.246 (1) Å; Co–S(2) = 2.230 (1) Å; and Co–S (2′) = 2.272 (1) Å. These bond distances are all shorter than the sum of the Co and S covalent radii, 2.28 Å.[23] All of the Co–S bonds in II are longer than those in I (2.113 (3) Å ⟨average⟩), which is at least partly a result of the change in the coordination number of cobalt.

It is interesting to note that the Co–S bond distances in II resemble those in the cubane-like cluster $[(\eta^5\text{-}C_5H_5)CoS]_4$[24] (V),

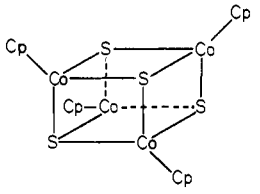

V

which average 2.230 Å. Several additional comparisons between II and V are noteworthy: II, ⟨average⟩ S–Co–S = 88.7 (1)°, V, ⟨average⟩ S–Co–S = 84.3 (1)°; II, Co–S(2)–Co = 93.94 (4)°, V, ⟨average⟩ Co–S–Co = 95.3 (1)°; the dihedral angle between the Cp plane and the S(1)–S(2)–S(2′) plane in II is 2.9°, and the average of the two equivalent planes[25] in V is 2.8°.

I and II can be distinguished by the IR absorptions in the 820–850-cm^{-1} region (vide supra), but ^{59}Co nuclear quadrupole resonance (NQR) spectroscopy provides a more decisive discrimination. Compound I possesses a *cis*-a_3b_2 ligand arrangement if the Cp ring is considered to be tridentate.[21] The coordination sphere of II is formally *fac*-a_3b_2c.[26] A significant difference in the electric field gradient at Co is produced in these two geometries.[27] Table VIII summarizes the coupling constants, e^2Qq/h, and asymmetry parameters, η, for ^{59}Co. The smaller values of e^2Qq/h and η in II are in line with the more space-filled coordination sphere and, perhaps, a shift in the principal axes of the electric field gradient tensor compared to I.[28] A similar decrease in the ^{59}Co NQR coupling constant is witnessed in pentacoordinate $(\eta^5\text{-}C_5H_5)Co(CO)_2$ (154 MHz)[21] compared to hexacoordinate $(\eta^5\text{-}C_5H_5)Co(CO)_2HgBr_2$ (108 MHz).[26] The difference in the electric field gradient of I and II is much larger than that which occurs with a simple first-order phase transition. The pairs of resonances obtained for I result from crystallographic inequivalence of the cobalt atoms. The frequency differences generated by the two sites is typical of the magnitude of change that takes place between two polymorphs involved in a first-order solid-phase transformation.

Characterization of the Reaction. The reversible conversion of I to II takes place in the solid phase with retention of the $P2_1/c$ space group. Because a crystallographic relationship appears to exist in the molecular positions of I and II, the reaction may be characterized as a displacement of the molecules in I toward one another, essentially along the *b*-axis of I, yielding a 6% increase in density. The orientation of the *b*-axis is not the same in I and II so the reaction is not topotactic. Accompanying the formation of new Co–S bonds, which raises the cobalt atom coordination number from five to six, is movement by both the cyclopentadienyl rings and the phenylene portion of the molecule. In the transformation of I to II at room temperature, the unit cell approximately halves in size, while *Z* drops from 8 to 2. The less dense solid, I, spontaneously converts to the more dense solid, II, as is expected for a thermodynamically favored transformation over a certain temperature range. The conversion is slow at 25 °C owing to a relatively rigid potential energy surface in the solid phase as well as to the probable need for defects to act as nucleation sites. By using rapid-scan FT-IR spectroscopy, the reverse transformation of II to I can be studied. Although the transformation rate is particle size dependent, it occurs sluggishly at about 150 °C but rapidly above this temperature. DSC measurements reveal that ΔH for II → I is +18.9 kJ mol^{-1} at 150–160 °C. This relatively small enthalpy change is similar to the values found in conformational polymorphism[29] and is small enough to account for the reversibility of this single-crystal chemical reaction. Despite the large amount of atomic movement, the energy factors are adventitiously balanced. The energetic similarity of I and II in the solid state is further manifested in the observation that dissolution of II in organic solvents, such as benzene, hexane, methylene chloride, and acetone, produces I as evidenced by the UV–vis spectrum. The dimer, II, is, therefore, the thermodynamically favored form in the crystal lattice at room temperature, but I is favored in solution.

The reversible dimerization of $(\eta^5\text{-}C_5H_5)Co(S_2C_6H_4)$ in the solid phase appears to hinge on a fortuitous balance of crystal and molecular forces. The Rh analogue of I is reported to be dimeric with no mention of a monomeric form.[30] We have observed that analogues of I, such as $(\eta^5\text{-}C_5H_5)Co(S_2C_2R_2)$ (R = CN, CF_3, H), $(\eta^5\text{-}C_5H_5)Co(O_2C_6H_4)$, $(\eta^5\text{-}C_5H_5)Co[(NH)_2C_6H_4]$, and $(\eta^5\text{-}C_5H_5)CpCo[(NH)SC_6H_4]$, do not dimerize in the solid state.[21]

Acknowledgment. The purchase of the X-ray diffractometer was supported in part by a grant from the National Science Foundation.

Registry No. I, 86409-56-5; II, 87739-02-4.

Supplementary Material Available: Tables of H atom positions, thermal parameters, and structure factors (32 pages). Ordering information is given on any current masthead page.

(23) Pauling, L. "The Nature of the Chemical Bond"; Cornell University Press: Ithaca, NY, 1960.
(24) Simon, G. L.; Dahl, L. F. *J. Am. Chem. Soc.* **1973**, *95*, 2164.
(25) Calculated by us from data in ref 24.
(26) Brill, T. B.; Landon, S. J.; Towle, D. K. *Inorg. Chem.* **1982**, *21*, 1437–1441.
(27) Brill, T. B. *J. Mol. Struct.*, in press.
(28) Brill, T. B.; Landon, S. J., to be published.
(29) Kitaigorodsky, A. I. "Molecular Crystals and Molecules"; Academic Press: New York, 1973; pp 10–62.
(30) Espinet, P.; Bailey, P. M.; Maitlis, P. M. *J. Chem. Soc., Dalton Trans.* **1979**, 1542–47.